

University of Groningen

Size-dependent ion-beam-induced anisotropic plastic deformation at the nanoscale by nonhydrostatic capillary stresses

van Dillen, T.; van der Giessen, E.; Onck, P. R.; Polman, A.

Published in:
Physical Review. B: Condensed Matter and Materials Physics

DOI:
[10.1103/PhysRevB.74.132103](https://doi.org/10.1103/PhysRevB.74.132103)

IMPORTANT NOTE: You are advised to consult the publisher's version (publisher's PDF) if you wish to cite from it. Please check the document version below.

Document Version
Publisher's PDF, also known as Version of record

Publication date:
2006

[Link to publication in University of Groningen/UMCG research database](#)

Citation for published version (APA):
van Dillen, T., van der Giessen, E., Onck, P. R., & Polman, A. (2006). Size-dependent ion-beam-induced anisotropic plastic deformation at the nanoscale by nonhydrostatic capillary stresses. *Physical Review. B: Condensed Matter and Materials Physics*, 74(13), [132103]. <https://doi.org/10.1103/PhysRevB.74.132103>

Copyright

Other than for strictly personal use, it is not permitted to download or to forward/distribute the text or part of it without the consent of the author(s) and/or copyright holder(s), unless the work is under an open content license (like Creative Commons).

The publication may also be distributed here under the terms of Article 25fa of the Dutch Copyright Act, indicated by the "Taverne" license. More information can be found on the University of Groningen website: <https://www.rug.nl/library/open-access/self-archiving-pure/taverne-amendment>.

Take-down policy

If you believe that this document breaches copyright please contact us providing details, and we will remove access to the work immediately and investigate your claim.

Downloaded from the University of Groningen/UMCG research database (Pure): <http://www.rug.nl/research/portal>. For technical reasons the number of authors shown on this cover page is limited to 10 maximum.

Size-dependent ion-beam-induced anisotropic plastic deformation at the nanoscale by nonhydrostatic capillary stresses

T. van Dillen,^{1,2} E. van der Giessen,² P. R. Onck,² and A. Polman¹

¹FOM-Institute for Atomic and Molecular Physics, Kruislaan 407, NL-1098 SJ Amsterdam, The Netherlands

²Materials Science Centre, University of Groningen, Nijenborgh 4, NL-9747 AG Groningen, The Netherlands

(Received 28 August 2006; published 18 October 2006)

We develop a phenomenological model for *size-dependent* anisotropic plastic deformation of colloidal nanoparticles under ion irradiation. We show that, at the nanoscale, nonhydrostatic capillary stresses drive radiation-induced Newtonian viscous flow, counteracting the stress state that initiates the anisotropic viscous strains in the high-temperature thermal spike region around the ion track. We present experimental data using colloidal silica nanoparticles in the 10–100 nm size range that show that the deformation is indeed strongly size dependent, in excellent agreement with the model. This work allows for the prediction of the ion-beam-induced shape modification of a whole range of nanostructures.

DOI: 10.1103/PhysRevB.74.132103

PACS number(s): 61.82.Ms, 61.43.-j, 61.80.-x, 82.70.Dd

Ion-irradiation-induced anisotropic plastic deformation was discovered in the early 1980s by Cartz *et al.*¹ They found that small amorphous silicate particles undergo an irradiation deformation process that elongates the particles in the direction perpendicular to the ion beam. More detailed studies of this phenomenon on thin films of metallic or silica glasses (5–15 μm thickness) were carried out later by Klaumünzer and coworkers.^{2–5} The anisotropic deformation originates from a shear transformation that occurs in the cylindrically shaped viscous ion-track region when it is rapidly heated (time scale ~ 10 ps, temperature several 1000 K). For the high ion energies used, the so-called thermal spike results from electronic excitations of the target atoms close to the ion track.^{6,7}

Recently, we have used colloidal particles as a microscopic model system for anisotropic deformation.⁸ Their perfect spherical shape and the fact that they can be deposited well separated from each other and imaged at high resolution have enabled a series of studies that have provided detailed information on the energy and temperature dependence of the anisotropic deformation.⁹ Both oblate and prolate ellipsoidal particle shape transformations were demonstrated,⁸ as well as shape changes in rectangular silicon micropillars.¹⁰ Most recently, we demonstrated how this ion-irradiation technique can be used to tune the geometry of colloidal masks for nanolithography.¹¹

At the nanoscale, capillary stresses become of the same order of magnitude as the stresses that drive anisotropic deformation. Capillary stresses drive stress relaxation that is mediated by Newtonian viscous flow, the latter being caused by ion-beam-induced atomic collisions.¹² A study of the size dependence of anisotropic deformation at the nanoscale may therefore provide a deeper insight into the fundamental phenomena that occur in the highly nonequilibrium thermal spike during ion irradiation.

Figure 1 shows a characteristic scanning electron microscope (SEM) image (10° tilt with substrate surface) of an originally spherical SiO_2 colloid (dashed circle), irradiated with 4 MeV Xe^{4+} ions at an angle of 45° with respect to the substrate normal, to a fluence of $4 \times 10^{14} \text{ cm}^{-2}$, and at a temperature of 85 K. As can be clearly seen, the colloid has

expanded perpendicular to the ion beam and contracted parallel to this direction. The observed aspect ratio (major over minor diameter) from this image is ~ 2 . Investigation of an ensemble of many particles (typically more than ten) has revealed that the average volume of the colloids has remained constant after irradiation.⁸

Trinkaas and Ryazanov have successfully described the deformation process at the ion-track scale by a viscoelastic thermal spike model in which local viscous strains, generated during relaxation of the constrained deviatoric (i.e., shear) thermal stress state, freeze upon rapid cooling of the spike, leading to a net expansion perpendicular to the ion track and a concomitant contraction along this direction.¹³ Recently, we have expanded this model by incorporating the time dependence of this relaxation process.¹⁴

The macroscopic anisotropic deformation can be described by a phenomenological model that was first proposed by Klaumünzer *et al.*^{15,16} In this model the macroscopic deformation, quantified by the Eulerian strain tensor $\underline{\epsilon}$ with components ϵ_{ij} ($i, j = 1, 2, 3$), is governed by the constitutive equation

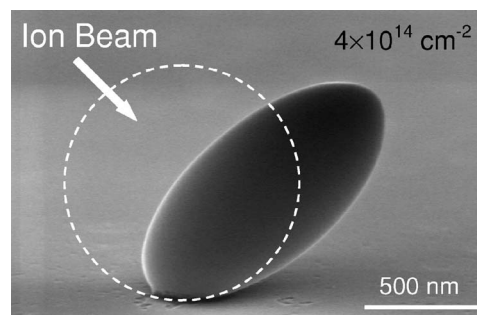


FIG. 1. Side-view scanning electron microscope image (10° tilt angle with respect to substrate surface) of a colloidal silica particle after irradiation with 4 MeV Xe^{4+} ions to a fluence of $4 \times 10^{14} \text{ cm}^{-2}$ at 85 K. Particles were irradiated at an angle of 45° with respect to the substrate surface normal as indicated by the white arrow. The dashed circle indicates the original size and location of the unirradiated colloid.

$$\frac{d\varepsilon_{ij}}{dt} \equiv \dot{\varepsilon}_{ij} = \frac{1}{2\mu} \frac{d}{dt} \left[\sigma_{ij} - \frac{\nu}{1+\nu} \sigma_{kk} \delta_{ij} \right] + \frac{1}{2\eta} \left[\sigma_{ij} - \frac{1}{3} \sigma_{kk} \delta_{ij} \right] + A_{ij}^0 \frac{d\Phi}{dt}, \quad (1)$$

where μ and ν are the shear modulus and Poisson's ratio of the irradiated material, respectively. The macroscopic stress tensor is $\underline{\sigma}$ with components σ_{ij} , where $\frac{1}{3}\sigma_{kk} = \frac{1}{3}(\sigma_{11} + \sigma_{22} + \sigma_{33})$ is the hydrostatic stress (the Einstein summation convention is used over repeated indices), δ_{ij} is the Kronecker delta ($\delta_{ij}=1$ for $i=j$, $\delta_{ij}=0$ for $i \neq j$), and $d\Phi/dt$ is the ion-beam flux (ions/cm² s). The first term on the right-hand side of Eq. (1) is Hooke's law for isotropic elastic media. The second term describes the macroscopic irradiation-induced Newtonian viscous behavior of the material with an ion-flux-dependent shear viscosity η , so that $\eta^{-1} \propto d\Phi/dt$. The last term on the right-hand side of Eq. (1) describes the unconstrained anisotropic deformation process and is given by

$$A_{ij}^0 = A_0(\delta_{ij} - 3b_i b_j). \quad (2)$$

Here A_0 is the strain increment per unit fluence in the absence of macroscopic stresses and b_i are the components of the unit vector \mathbf{b} along the ion beam. By means of this model [i.e., Eqs. (1) and (2) and the relation between the rate-of-strain tensor and the velocity components], the anisotropic deformation of spherical colloidal silica particles of 300 nm and 1 μm in diameter under 4 MeV Xe ion irradiation is successfully described.¹⁷ The model also describes the fluence dependence of the principal diameters of the colloids as well as a fluence-dependent angular roll-off.¹⁸

In the previous analyses, the influence of capillary stresses σ_{ij} due to surface curvature was not taken into account. This was justified by the fact that the colloids used were relatively large. Here, we show that stresses by surface curvature play a key role in the anisotropic deformation of colloidal nanoparticles with diameters smaller than 100 nm. Spherical silica colloids with radii of 19 nm made using a microemulsion method,¹⁹ and colloids with radii of 46, 153, and 510 nm synthesized using techniques described in Refs. 20 and 21, were irradiated with 4 MeV Xe ions to fluences in the range between $1 \times 10^{14} \text{ cm}^{-2}$ and $1 \times 10^{15} \text{ cm}^{-2}$ at 85 K at an angle of 45°. Figure 2 shows the transverse diameter L ,²² normalized with the initial colloid diameter $2R$, as a function of the ion fluence Φ . Clearly, for small fluences ($< 2 \times 10^{14} \text{ Xe/cm}^2$), the anisotropic deformation is not size dependent. However, at higher ion fluences, smaller colloids show less deformation than larger colloids. For example, at a fluence of $1 \times 10^{15} \text{ Xe/cm}^2$, $L/(2R)$ increases with colloid size from 1.29 for 46-nm-radius colloids to 1.71 for 510-nm-radius colloids. The size dependence of $L/(2R)$ at a fixed fluence of $4 \times 10^{14} \text{ Xe/cm}^2$ is shown in Fig. 3; it gradually increases from 1.12 for very small colloids of 19 nm radius, to 1.29 for 510-nm-radius colloids. It can be seen that the size dependence of the deformation becomes most pronounced for colloid radii < 100 nm.

In the absence of a macroscopic contribution to the stresses σ_{ij} , the fluence dependence of the anisotropic deformation

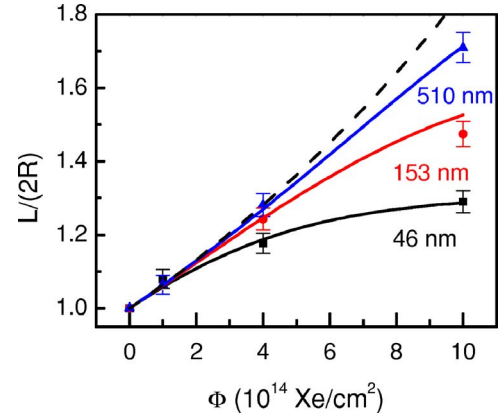


FIG. 2. (Color online) The measured transverse diameter L , normalized with the original diameter $2R$, as a function of ion fluence Φ for colloidal particles with mean radius $R=46$ nm (black squares), 153 nm (red circles), and 510 nm (blue triangles), respectively. The black dashed line is the initial, exponential growth behavior for free anisotropic plastic deformation with $A_0=6.2 \times 10^{-16} \text{ cm}^2/\text{ion}$. The solid lines [$R=46$ nm (black), 153 nm (red), and 510 nm (blue)], are calculated curves using Eq. (6) from the proposed phenomenological model with $\eta_{\text{RAD}}=9.0 \times 10^{21} \text{ Pa ion/cm}^2$.

can be calculated from Eqs. (1) and (2). If we take the ion beam along the x_3 axis, i.e., $b_1=b_2=0$ and $b_3=1$, the strain increments per unit fluence in the direction perpendicular to the ion beam (1,2 directions) are $d\varepsilon_{11}/d\Phi = d\varepsilon_{22}/d\Phi = dL/(Ld\Phi) = A_0$.²³ This differential equation leads to an exponential growth of $L/(2R)$ with fluence Φ : $L(\Phi)/(2R) = \exp[A_0\Phi]$ as is plotted in Fig. 2 with $A_0=6.2 \times 10^{-16} \text{ cm}^2/\text{ion}$ (black, dashed curve).¹⁷ As can be seen, for small fluences this growth curve describes the experimental data well for all used colloid sizes. The deviation from this curve for data at higher fluences indicates that macroscopic stresses σ_{ij} cannot be ignored in describing ion-irradiation-induced anisotropic deformation and that the first two terms on the right-hand side of Eq. (1) must also be taken into account to describe the deformation.

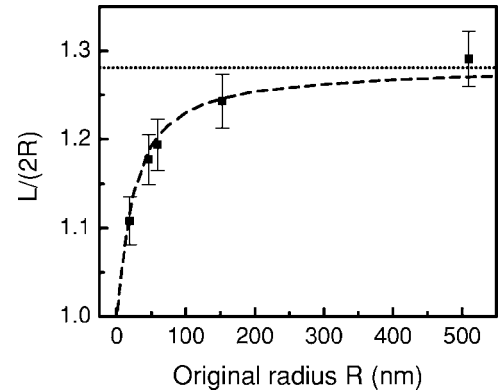


FIG. 3. The measured transverse diameter L , normalized with the original diameter $2R$, as a function of the original colloid radius R , measured after irradiation at $4 \times 10^{14} \text{ Xe/cm}^2$ (solid squares). The dashed curve is a calculation using Eq. (6) with $A_0=6.2 \times 10^{-16} \text{ cm}^2/\text{ion}$ and $\eta_{\text{RAD}}=9.0 \times 10^{21} \text{ Pa ion/cm}^2$. The dotted horizontal line is the limiting value of $L/(2R)$ for large R .

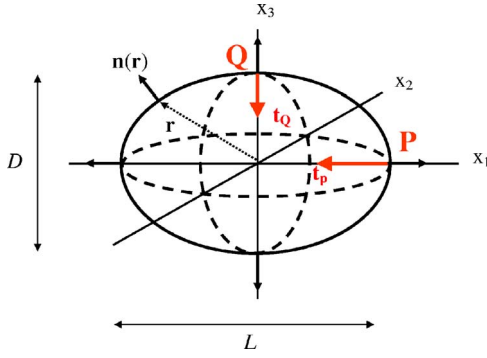


FIG. 4. (Color online) Schematic of an oblate spheroid of major diameter L and minor diameter D . At a position \mathbf{r} at the surface of the oblate the normal is $\mathbf{n}(\mathbf{r})$ is indicated by the black arrows. The traction vectors \mathbf{t}_P and \mathbf{t}_Q (resulting from surface curvature) at points P and Q , respectively, are indicated by red arrows.

Based on the experimental results presented in Figs. 2 and 3 we hypothesize that stresses resulting from surface curvature are the origin of the observed size dependence. At a point \mathbf{r} at the surface of the (oblate) colloid having surface normal \mathbf{n} (with components n_k), as sketched in Fig. 4, the surface traction components $t_i(\mathbf{r}) = \sigma_{ik}(\mathbf{r})n_k(\mathbf{r})$ are given by Laplace's formula

$$\sigma_{ik}(\mathbf{r})n_k(\mathbf{r}) = -\gamma \left(\frac{1}{R_{\min}(\mathbf{r})} + \frac{1}{R_{\max}(\mathbf{r})} \right) n_i(\mathbf{r}), \quad (3)$$

where γ is the specific surface energy, and $R_{\min}(\mathbf{r})$ and $R_{\max}(\mathbf{r})$ are the minimum and maximum radii of curvature, respectively. In case of a spherical particle of radius R the surface stress is normal to and uniform over the colloid's surface; this induces a uniform hydrostatic stress $\sigma_{11} = \sigma_{22} = \sigma_{33} = -2\gamma/R$ inside the colloid. However, in case of an oblate particle with major diameter L and minor diameter D , as in the sketch of Fig. 4, the traction according to Eq. (3) will vary over the surface. The resulting stress state inside the colloid is not known and not trivial. As a first estimate of the surface tension effect, we assume that all stress components σ_{ij} are uniform. Then, because of axisymmetry about the principal axes of the colloid, $\sigma_{12} = \sigma_{13} = \sigma_{23} = 0$ and $\sigma_{11} = \sigma_{22}$. In point P where the x_1 axis crosses the surface (see Fig. 4) and $\mathbf{n} = (1, 0, 0)$, Eq. (3) allows us to calculate the stress component σ_{11} . Then, with $R_{\min} = \frac{1}{2}D^2/L$ and $R_{\max} = L/2$, we obtain

$$\sigma_{11} = -2\gamma \frac{1 + (D/L)^2}{L (D/L)^2}. \quad (4)$$

Similarly, in point Q where $\mathbf{n} = (0, 0, 1)$ and $R_{\min} = R_{\max} = \frac{1}{2}L^2/D$, we find

$$\sigma_{33} = -4\gamma \frac{1}{L} \left(\frac{D}{L} \right). \quad (5)$$

We can evaluate these stresses taking the specific surface energy for hydroxyl-terminated silica ($\gamma = 0.4 \text{ J/m}^2$) (Ref. 24) and first determine the average elastic strain rate contribution (averaged over the duration of the irradiation) to Eq.

(1). For the smallest colloids ($R = 19 \text{ nm}$) irradiated to the highest fluence ($1 \times 10^{15} \text{ Xe/cm}^2$), the average elastic strain increment per unit ion fluence perpendicular to the ion beam (i.e., $d\epsilon_{11}/d\Phi = d\epsilon_{22}/d\Phi$) is on the order of $10^{-19} \text{ cm}^2/\text{ion}$, three to four orders of magnitude smaller than the value A_0 for anisotropic deformation. We can therefore ignore the first term (elastic contribution) in Eq. (1) and only take into account Newtonian viscous flow with shear viscosity η , driven by deviatoric stresses $s_{ij} = \sigma_{ij} - \frac{1}{3}\sigma_{kk}\delta_{ij}$.

The viscous strain rate, $s_{ij}/(2\eta)$, can now be calculated using Eqs. (4) and (5). With the ion beam along the x_3 axis, the total strain rate perpendicular to the ion beam (from Eq. (1) can be rewritten as a differential equation for the transverse axis L of the colloidal particle, resulting in²³

$$\frac{dL}{d\Phi} = A_0 L - \frac{\gamma}{6\eta_{\text{RAD}}} \left[2 + \frac{L^6}{32R^6} - 32\frac{R^3}{L^3} \right]; \quad L(\Phi = 0) = 2R, \quad (6)$$

where we have used $D = 8(R^3/L^2)$ expressing volume conservation²⁵ and defined $\eta_{\text{RAD}} \equiv \eta(d\Phi/dt)$, the ion-flux independent radiation-induced viscosity.^{12,26,27} The first term in Eq. (6) describes the free deformation in absence of stresses (exponential growth). The second term describes Newtonian viscous flow resulting from stresses by surface curvature. At small fluences, particles are still close to spherical ($L \approx 2R$), and the second term in Eq. (6) is negligible. The anisotropic deformation, $L/(2R)$, of each particle therefore starts at a constant rate A_0 , irrespective of its radius R . As the anisotropic deformation process continues, the anisotropy in surface stress (quantified by the deviatoric stress) increases and the second, negative term in Eq. (6) becomes significant. Newtonian viscous flow then counteracts the net anisotropic deformation per unit fluence and the transverse diameter L deviates from its exponential growth behavior and finally saturates when $dL/d\Phi = 0$.

Based on this viscoelastic model, we can fit all experimental data in Figs. 2 and 3 by numerically solving Eq. (6) with a single set of fitting parameters A_0 and η_{RAD} . The drawn curves in Figs. 2 and 3 give the best results, with $A_0 = (6.2 \pm 0.2) \times 10^{-16} \text{ cm}^2/\text{ion}$ and $\eta_{\text{RAD}} = (0.90 \pm 0.05) \times 10^{22} \text{ Pa ion/cm}^2$. The dotted horizontal line in Fig. 3 is the limiting value for $R \rightarrow \infty$ of the calculated curve. As can be seen, the theoretical model captures all experimental data in detail. We therefore conclude that a nonhydrostatic stress distribution by surface curvature is the dominant factor in limiting the anisotropic deformation effect.

Note that the value of A_0 is similar to what we found previously for colloidal silica particles under 4 MeV Xe irradiation.^{8,17} The value found for η_{RAD} is about one order of magnitude smaller than the value measured for thermally grown silica using *in situ* wafer curvature measurements during ion irradiation.^{12,26,27} Indeed, colloidal silica is a relatively "soft" material, with a lower bulk melting point than thermal SiO_2 and thus is expected to have a lower viscosity. Direct measurements of the radiation-induced viscosity of colloidal silica are lacking, but conversely, the fitted value for η_{RAD} found here may serve as its first determination. At the presently used ion flux, the found value for η_{RAD} trans-

lates to a shear viscosity η of about 1.5×10^{11} Pa s.

In conclusion, the anisotropic deformation of submicron-sized colloidal particles under ion irradiation is strongly size dependent. While the incremental anisotropic strain per unit fluence, A_0 , remains constant for all radii between 19 nm and 510 nm, the particle anisotropy decreases with decreasing size. This is the result of an increased deviatoric capillary stress state at smaller sizes, in combination with radiation-induced Newtonian viscous flow. The data compare well with a phenomenological, macroscopic deformation model that takes into account the nonhydrostatic stresses by surface curvature, and yields a strain increment per unit fluence $A_0 = 6.2 \times 10^{-16}$ cm²/ion for anisotropic deformation and a

radiation-induced shear viscosity $\eta_{\text{RAD}} = 0.90 \times 10^{22}$ Pa ion/cm². This is the first demonstration that size does matter during ion irradiation, and demonstrates the intricate interplay between radiation-induced viscous flow, anisotropic strain generation, and capillary stresses.

The authors thank B. M. Mulder and D. Frenkel (FOM-Institute AMOLF) for fruitful discussions. A. van Blaaderen and C. M. van Kats (University of Utrecht) are gratefully acknowledged for supplying colloidal particles. This work is part of the research program of FOM and was financially supported by NWO.

-
- ¹L. Cartz, F. G. Karioris, and R. A. Fournelle, *Radiat. Eff.* **54**, 57 (1981).
- ²S. Klaumünzer and G. Schumacher, *Phys. Rev. Lett.* **51**, 1987 (1983).
- ³S. Klaumünzer, M. D. Hou, and G. Schumacher, *Phys. Rev. Lett.* **57**, 850 (1986).
- ⁴M. D. Hou, S. Klaumünzer, and G. Schumacher, *Phys. Rev. B* **41**, 1144 (1990).
- ⁵L. Thomé, F. Garrido, J. C. Dran, A. Benyagoub, S. Klaumünzer, and A. Dunlop, *Phys. Rev. Lett.* **68**, 808 (1992).
- ⁶M. Toulemonde, C. Dufour, and E. Paumier, *Phys. Rev. B* **46**, 14362 (1992).
- ⁷M. Toulemonde, Ch. Dufour, E. Paumier, and F. Pawlak, *Mater. Res. Soc. Symp. Proc.* **504**, 99 (1999).
- ⁸E. Snoeks, A. van Blaaderen, C. M. van Kats, M. L. Brongersma, T. van Dillen, and A. Polman, *Adv. Mater. (Weinheim, Ger.)* **12**, 1511 (2000).
- ⁹T. van Dillen, A. Polman, C. M. van Kats, and A. van Blaaderen, *Appl. Phys. Lett.* **83**, 4315 (2003).
- ¹⁰T. van Dillen, M. J. A. de Dood, J. J. Penninkhof, A. Polman, S. Roorda, and A. M. Vredenberg, *Appl. Phys. Lett.* **84**, 3591 (2004).
- ¹¹D. L. J. Vossen, D. Fific, J. J. Penninkhof, T. van Dillen, A. Polman, and A. van Blaaderen, *Nano Lett.* **5**, 1175 (2005).
- ¹²E. Snoeks, T. Weber, A. Cacciato, and A. Polman, *J. Appl. Phys.* **78**, 4723 (1995).
- ¹³H. Trinkaus and A. I. Ryazanov, *Phys. Rev. Lett.* **74**, 5072 (1995).
- ¹⁴T. van Dillen, A. Polman, P. R. Onck, and E. van der Giessen, *Phys. Rev. B* **71**, 024103 (2005).
- ¹⁵S. Klaumünzer and A. Benyagoub, *Phys. Rev. B* **43**, 7502 (1991).
- ¹⁶A. Gutzmann, S. Klaumünzer, and P. Meier, *Phys. Rev. Lett.* **74**, 2256 (1995).
- ¹⁷S. Klaumünzer, *Nucl. Instrum. Methods Phys. Res. B* **215**, 345 (2004).
- ¹⁸During ion irradiation the colloid undergoes an apparent rotation; the angle between the colloid's major axis and the substrate gradually decreases (angular roll-off), see T. van Dillen, Ph.D. thesis, Utrecht University, 2004, URL: <http://www.amolf.nl/>; and Ref. 17.
- ¹⁹K. Osseo-Asare and F. J. Arriagada, *Colloids Surf.* **50**, 321 (1990).
- ²⁰A. van Blaaderen, J. van Geest, and A. Vrij, *J. Colloid Interface Sci.* **154**, 481 (1992).
- ²¹A. van Blaaderen and A. Vrij, *Langmuir* **8**, 2921 (1992).
- ²² L is the diameter perpendicular to the ion beam at every stage during the irradiation; this major axis is not affected by the angular roll-off effect.
- ²³We have used $d\Phi = (d\Phi/dt)dt$ in Eq. (1).
- ²⁴H. Scholze, *Glass* (Springer-Verlag, New York, 1991).
- ²⁵The small effect of angular roll-off was ignored here and a purely oblate ellipsoidal shape was assumed.
- ²⁶E. Snoeks, A. Polman, and C. A. Volkert, *Appl. Phys. Lett.* **65**, 2487 (1994).
- ²⁷M. L. Brongersma, E. Snoeks, and A. Polman, *Appl. Phys. Lett.* **71**, 1628 (1997).